

Dispersion relation for the linear theory of relativistic Rayleigh–Taylor instability in magnetized medium revisited

Qiqi Jiang^{1,2,3*}, Guang-Xing Li^{1**}, and Chandra B. Singh^{1***}

¹ South-Western Institute for Astronomy Research, Yunnan University, Kunming, 650500 Yunnan, P.R. China

² Deutsches Elektronen-Synchrotron DESY, Platanenallee 6, 15738 Zeuthen, Germany

³ Institute of Physics and Astronomy, University of Potsdam, 14476 Potsdam, Germany

ABSTRACT

Context. The Rayleigh–Taylor instability (RTI) arises at the interface between two fluids of different densities, notably when a heavier fluid lies above a lighter one in an effective gravitational field. In astrophysical systems with high velocities, relativistic corrections are essential, and special relativity provides a practical framework to describe such dynamics, introducing a unified space-time perspective. This interplay of classical fluid instability and relativistic effects is significant in astrophysics, impacting systems where fluid motion approaches relativistic speeds.

Aims. We investigate the linear theory of relativistic Rayleigh–Taylor instability (R-RTI) in a magnetized medium, where fluids can move parallel to the interface at relativistic velocities. This study aims to understand how relativistic effects modify the classic RTI in the presence of a horizontal magnetic field and to derive conditions under which the instability is activated.

Methods. To simplify our analysis, we chose an "intermediate frame" where fluids on each side of the interface move in opposite directions with identical Lorentz factors. This symmetry facilitates analytical derivations and the study of relativistic effects on the instability's dynamics.

Results. Our results indicate that the instability is activated when the Atwood number $\mathcal{A} = (\rho_1 h_1 - \rho_2 h_2) / (\rho_1 h_1 + \rho_2 h_2) > 0$, where no relativistic correction is required. The relativistic motion can increase the effective inertia of the gas ($\rho \rightarrow \gamma^2 \rho$), weakening the effect of the horizontal magnetic field in suppressing the instability. When observed in the laboratory frame, the growth rate of the instability is significantly reduced due to time dilation. The analytical results should guide further explorations of instability in systems such as microquasars (μ QSOs), Active galactic nuclei (AGNs), gamma-ray bursts (GRBs), and radio pulsars (PSRs).

Key words. Instabilities — Magnetohydrodynamics (MHD) — Relativistic process — Jets

1. Introduction

Special relativity (Taylor & Wheeler 1992), a cornerstone of 20th-century physics, plays a critical role in understanding the behavior of fluids moving at speeds close to the speed of light. This theory unifies space and time into a single entity, a concept necessary for describing relativistic astrophysical phenomena. Understanding relativistic fluids (Landau & Lifshitz 1987) has become a crucial challenge with the advancement of high-energy astrophysics. Our specific topic is to study the evolution of Rayleigh–Taylor instabilities in the relativistic context.

The Rayleigh–Taylor instability (RTI) is one fundamental macroscopic instability in nature (Chandrasekhar 1961; Sharp 1984). It occurs at the interface between two different densities of fluids and becomes activated when the density gradient is in the opposite direction of the overall acceleration. The growth of the RTI can disrupt the stability of the interface, leading to subsequent mixing between two fluids, often in the form of some finger-bubble structures. The core of the theory of the RTI is the key part of other instabilities, including the Centrifugal Instability (CFI) (Gourgouliatos & Komissarov 2018) and the Richtmyer–Meshkov instability (RMI) (Kane et al. 1999; Wilder & Richtmyer 1954), where the effective acceleration is provided either by rotation (CFI) or by acceleration from a impulse (RMI).

In an astrophysical jet, the growth of these instabilities can lead to mixing between the jet and the ambient medium, leading to the deceleration of the jet. In supernova explosions, the region between the forward shock in the interstellar medium and the reverse shock in the ejecta is RT unstable (Wang & Chevalier 2001), and the growth of the instabilities can lead to mixing and energy dissipation. Numerical simulation of 3D RTI in supernova remnants studies the effect of efficient particle acceleration at the forward shock on the growth of RTI (Fraschetti et al. 2010). The particle-in-cell (PIC) simulation of particle acceleration by magnetic RTI is performed and explains flares from the inner accretion flow onto the supermassive black hole, Sgr A* (Zhdankin et al. 2023).

Since most astrophysical plasma is magnetized, the inclusion of the effect of the magnetic field is required. Some previous works about the magnetic RTI have been done (Hillier 2016, 2018), which mainly discuss the most unstable modes of the system in the linear stage of its evolution and this instability develops in solar prominences. Matsumoto et al. (2017) investigated the linear evolution theory of non-magnetized RTI at a discontinuous surface between a relativistic jet and a cocoon. Despite the widespread acceptance, the results are not correct, which is evidenced by its breakdown under a simple Lorentz transformation (Sec. 2).

In this paper, we provide the correct form of the dispersion relation for R-RTI in the magnetized medium. Even though this study deals with relativistic systems, many of the core prin-

* E-mail: qiqi.jiang@desy.de

** E-mail: ligx.ngc7293@gmail.com

*** E-mail: chandrasingh@ynu.edu.cn

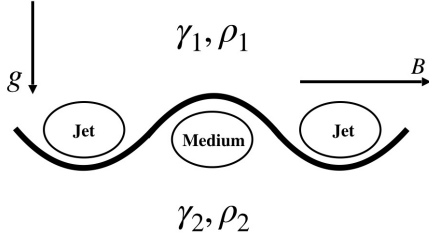


Fig. 1. Jet cross-section in the x - y plane.

Table 1. List of variables

\mathbf{B} : Magnetic field	μ : Magnetic permeability
\mathbf{g} : Acceleration vector	\mathcal{A} : Atwood number
ρ : Rest-mass density	k : Wavenumber
γ : Lorentz factor	ω : Frequency
h : Specific enthalpy	

principles discussed are highly relevant to the classical fluid dynamics community. The effects of fluid inertia, stability criteria, and magnetic field interactions, as derived in the relativistic regime, are universal features that appear in classical systems as well. Understanding how relativistic corrections alter these dynamics can deepen the comprehension of similar processes in non-relativistic fluid flows, particularly in extreme environments involving high velocities or strong gravitational influences. As such, this paper bridges the gap between relativistic and classical fluid dynamics, offering preliminary theoretical insights that can be applied to astrophysical systems. Our derivation is performed with the help of a new concept called the "intermediate frame" (Sec. 3), where fluids from both sides have the same Lorentz factor. This final form of the dispersion relation is presented in different frames (Sec. 4), and the astrophysical implications are discussed in Sec. 5.

2. Problem setup

We isolate the linear analysis of R-RTI in the magnetized medium by starting with the fluid box in Fig. 1. There are two fluids of densities ρ_1, ρ_2 and Lorentz factors γ_1, γ_2 , separated by an interface. \mathbf{g} is effective acceleration provided by restoring force caused by e.g. jet oscillation. The medium is magnetized with a uniform horizontal magnetic field along the x axis. The meanings of the variables are summarized in Table. 1.

2.1. Dispersion relation with some inconsistencies

Through the standard procedure of tracing the development of linear perturbation through a set of equations, we arrive at the following dispersion relation of relativistic magnetized RTI (See Appendix A for the detailed derivations):

$$\omega^2 = -gk \left\{ \frac{\gamma_1^2 \rho_1 h_1 - \gamma_2^2 \rho_2 h_2}{\gamma_1^2 \rho_1 h_1 + \gamma_2^2 \rho_2 h_2} - \frac{\mu B^2 k}{2\pi (\gamma_1^2 \rho_1 h_1 + \gamma_2^2 \rho_2 h_2) g} \right\}, \quad (1)$$

where

$$\mathcal{A}_{\text{incorrect}} = \frac{\gamma_1^2 \rho_1 h_1 - \gamma_2^2 \rho_2 h_2}{\gamma_1^2 \rho_1 h_1 + \gamma_2^2 \rho_2 h_2}. \quad (2)$$

is an incorrect version of the Atwood number in the non-magnetized relativistic regime.

The magnetized R-RTI sets in when $\omega^2 < 0$. This corresponds to the situation where the frequencies are imaginary such that the corresponding perturbations will grow exponentially.

However, we believe that this equation has obvious inconsistencies. We will expose the contradictions by observing the growth of the instability from two frames, with frame 1 following fluid 1 and frame 2 following fluid 2, respectively. The relative velocity is $\beta_{1,2}$ and the corresponding Lorentz factor is $\gamma_{1,2}$. The inconsistent nature of Eq. 1 can be seen from the fact that whether the instabilities can grow or not becomes dependent on the frame of choice:

In fluid 1 frame, $\beta_1 = 0$, $\gamma_1 = 1$. Whether the instability can grow is determined by the Atwood number, which is

$$\mathcal{A}_{\text{incorrect},1} = \frac{\rho_1 h_1 - \gamma_{1,2}^2 \rho_2 h_2}{\rho_1 h_1 + \gamma_{1,2}^2 \rho_2 h_2}, \quad (3)$$

and the fluid is unstable if

$$\rho_1 h_1 > \gamma_{1,2}^2 \rho_2 h_2. \quad (4)$$

However, in the fluid 2 frame, $\beta_2 = 0$, $\gamma_2 = 1$. Whether the instability can grow is determined by the Atwood number, which is

$$\mathcal{A}_{\text{incorrect},2} = \frac{\gamma_{1,2}^2 \rho_1 h_1 - \rho_2 h_2}{\gamma_{1,2}^2 \rho_2 h_2 + \rho_2 h_2}, \quad (5)$$

and the fluid is unstable if

$$\rho_2 h_2 < \gamma_{1,2}^2 \rho_1 h_1. \quad (6)$$

Eqs. 4 and 6 are inconsistent with each other. The Atwood number in Eq. 2 does not satisfy the Lorentz invariance and is not consistent. Here, we consider the positive wave with $k > 0$ for the above analysis.

3. Length contraction paradox

In most theoretical studies, the governing magnetic hydrodynamical equations are solved with a reduced number of dimensions. For example, in the case of the traditional RTI, one only needs to derive the dispersion relation in 1D, because the default situation is that all directions that are perpendicular to the interaction are identical.

Considering a small size perturbation, (l_x, l_y, l_z) . When $l_z \gg l_x$ and $l_z \ll l_y$, the system is invariant under the translation $z' = z + \delta z$. Due to the symmetry of 2D, we can neglect the z direction and analyze the system in the x - y plane. This approach has been widely adopted in the relativistic case but may cause problems with the system in the relativistic case.

3.1. The theory of length contraction paradox

The *length contraction paradox* refers to the case where one arrives at wrong results by solving the relativistic fluid equations with fewer dimensions. For example, solving the fluid equations in the x - y plane when the velocity along the z direction can lead to inconsistencies when the system contains relativistic velocities along the z direction.

To illustrate this inconsistency, we reconsider a perturbation of the size (l_x, l_y, l_z) measured at the observer's frame at the interface between two fluids. For the analysis to be consistent, its measured length should be the same for fluids in all three directions. In the non-relativistic case, the measured size is (l_x, l_y, l_z) for fluids in all possible frames, and there is no inconsistency.

In the relativistic case, the *length contraction* effect can introduce some additional constrains, which needs to be accounted for when formulating the problem. Assuming that fluid 1 has velocity $(0, 0, \beta_1)$, and fluid 2 has velocity $(0, 0, \beta_2)$. This perturbation measures to $(l_x, l_y, l_z \gamma(\beta_1)^{-1})$ in fluid 1's frame, and $(l_x, l_y, l_z \gamma(\beta_2)^{-1})$ in fluid 2's frame. The ratio between the measured length in two different frames along the z direction is

$$f = \frac{\gamma(\beta_2)}{\gamma(\beta_1)}, \quad (7)$$

which is not Lorentz invariant. The relativistic motion makes it no longer possible to drop the z direction from the analysis. This situation is illustrated in Fig. 2.

3.2. Simplifying the problem through the intermediate frame

A direct solution for the length contraction paradox is to solve the full, 3D relativistic magnetized R-RTI equations. However, this approach is time-consuming for simulations, and tedious to perform analytically. An easy shortcut to eliminate this inconsistency is to construct a proper reference frame. In the case of relativistic RTI, suppose fluid 1 has a velocity β_1 and Lorentz factor γ_1 , and fluid 2 has a velocity of β_2 and Lorentz factor γ_2 , we construct a *intermediate frame* where

$$\begin{aligned} \beta'_1 &= -\beta_{\text{intermediate}} \\ \beta'_2 &= \beta_{\text{intermediate}} \\ \gamma'_1 &= \gamma'_2 = \gamma(\beta_{\text{intermediate}}), \end{aligned} \quad (8)$$

where β'_1 and β'_2 are the velocities of fluid 1 and fluid 2 measured in the intermediate frame, and γ are the corresponding Lorentz factors.

Perturbations of size (l_x, l_y, l_z) measured in the intermediate frame have the same length of $(l_x, l_y, l_z \gamma_{\text{intermediate}}^{-1})$ seem from both the rest frame of fluid 1 and fluid 2. This smart choice of reference eliminates the inconsistency that has been discussed in 3.1. An illustration of this idea can be found in Fig. 2.

To derive the Lorentz factor of the intermediate frame, assuming that fluid 1 and fluid 2 have velocities of β_1 and β_2 respectively, using the formula for velocity addition, the velocity of fluid 1 measured in the intermediate frame is

$$\beta'_1 = \frac{\beta_1 - \beta_{\text{intermediate}}}{1 - \beta_{\text{intermediate}}\beta_1}, \quad (9)$$

and the velocity of fluid 2 measured in the intermediate frame is

$$\beta'_2 = \frac{\beta_2 - \beta_{\text{intermediate}}}{1 - \beta_{\text{intermediate}}\beta_2}. \quad (10)$$

Letting $\beta'_1 = -\beta'_2$, we have

$$\beta_* = \frac{\beta_1\beta_2 - \sqrt{\beta_1^2\beta_2^2 - \beta_1^2 - \beta_2^2 + 1 + 1}}{\beta_1 + \beta_2}, \quad (11)$$

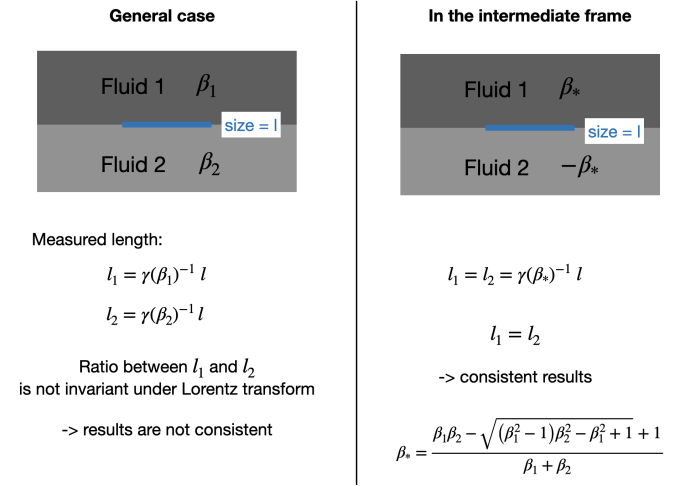


Fig. 2. A illustration of how to choose the appropriate reference frame to simplify the problem in relativistic hydrodynamics.

and

$$\gamma_* = \frac{1}{(1 - \beta_*^2)^{1/2}}, \quad (12)$$

where β_* is the uniform velocity of fluids in the intermediate frame and the γ_* is the corresponding uniform Lorentz factor.

A common use case of Eq. 11 is when we stay in the same frame as one of the fluids. In this case, assuming $\beta_2 = 0$, we have

$$\beta_* = \sqrt{\frac{\gamma_1 - 1}{\gamma_1 + 1}}, \quad (13)$$

and

$$\gamma_* = \sqrt{\frac{\gamma_1 + 1}{2}}. \quad (14)$$

where we focus on the highly relativistic case when $\gamma_1 \gg 1$.

4. Correction of dispersion relation of the R-RTI

4.1. The relativistic Atwood number

After establishing the concept of the intermediate frame, we can obtain the correct form of the dispersion dispersion for R-RTI. In the intermediate frame, we make the substitution of $\gamma_1 = \gamma_2 = \gamma_*$ into the Eq. 2, then we obtain the correction relativistic Atwood number:

$$\mathcal{A} = \frac{\rho_1 h_1 - \rho_2 h_2}{\rho_1 h_1 + \rho_2 h_2}. \quad (15)$$

The Eq. 15 shows the onset of the relativistic RTI is only determined by the density contrast $\rho_1 h_1 - \rho_2 h_2$. Here, we note that the strength of the magnetic field is small and its contribution to the specific enthalpy h can be ignored. This result is consistent, especially when compared to Matsumoto et al. (2017)'s version where $\gamma_1^2 \rho_1 h_1 - \gamma_2^2 \rho_2 h_2$.

4.2. Complete dispersion relation

4.2.1. Dispersion relation in the intermediate frame

In the intermediate frame, by substituting $\gamma_1 = \gamma_2 = \gamma_*$ to Eq. 1, the correction dispersion relation for the R-RTI is

$$\begin{aligned} \omega_{\text{intermediate}}^2 &= -gk_{\text{intermediate}} \left\{ \frac{\rho_1 h_1 - \rho_2 h_2}{\rho_1 h_1 + \rho_2 h_2} \right. \\ &\quad \left. - \frac{\mu B^2 k_{\text{intermediate}}}{2\pi(\rho_1 h_1 + \rho_2 h_2)g\gamma_*^2} \right\} \\ &= -gk_{\text{intermediate}} \left\{ \mathcal{A} - \frac{\mu B^2 k_{\text{intermediate}}}{2\pi(\rho_1 h_1 + \rho_2 h_2)g\gamma_*^2} \right\}. \end{aligned} \quad (16)$$

4.2.2. Full dispersion relation in the lab frame

We extend our results to make them applicable in arbitrary frames. To achieve this, we must take the *relativistic/apparent effects* such as time dilation and length contraction into account. By making the following substitutions

$$\begin{aligned} \omega_{z,\text{lab}} &= \gamma_*^{-1} \omega_{\text{intermediate}} \\ k_{z,\text{lab}} &= \gamma_* k_{z,\text{intermediate}}, \end{aligned} \quad (17)$$

we arrive at the correction dispersion relation of magnetized R-RTI:

$$\omega_{\text{lab}}^2 = -\frac{gk_{z,\text{lab}}}{\gamma_*^3} \left\{ \mathcal{A} - \frac{\mu B^2 k_{z,\text{lab}}}{2\pi(\rho_1 h_1 + \rho_2 h_2)g\gamma_*^3} \right\}. \quad (18)$$

γ_* is defined in Eq. 12.

5. Properties of the dispersion relation and relativistic effects

5.1. Condition for instability

According to our analysis, the system becomes unstable when $\mathcal{A} > 0$. According to Eq. 15, the instability sets in $\rho_1 h_1 > \rho_2 h_2$. Whether the instability can grow or not is determined by the density contrast alone, which is identical to the non-relativistic case as discussed in Chandrasekhar (1961). Contrary to the conclusion from Matsumoto et al. (2017), *parallel motion does not have effects on whether the instability will grow or not*.

5.2. Critical wavelength

In the non-relativistic case, the unstable modes have

$$k < k_{\text{crit,non-relativistic}} = \frac{2\pi g(\rho_1 h_1 - \rho_2 h_2)}{\mu B^2}, \quad (19)$$

where the effect of the uniform magnetic field is to suppress the growth of small-scale modes with large k .

In the magnetized R-RTI case, the unstable modes have

$$k < k_{\text{crit,intermediate}} = \gamma_*^2 \frac{2\pi g(\rho_1 h_1 - \rho_2 h_2)}{\mu B^2}, \quad (20)$$

which is measured in the intermediate frame. Compared to the non-relativistic case, the critical wave number is larger and the condition for instability is loosened. The results can be understood as follows: the relativistic motions lead to increases in the effective inertia ($\rho \rightarrow \gamma_*^2 \rho$), which makes it harder for the magnetic field to suppress the growth of the R-RTI.

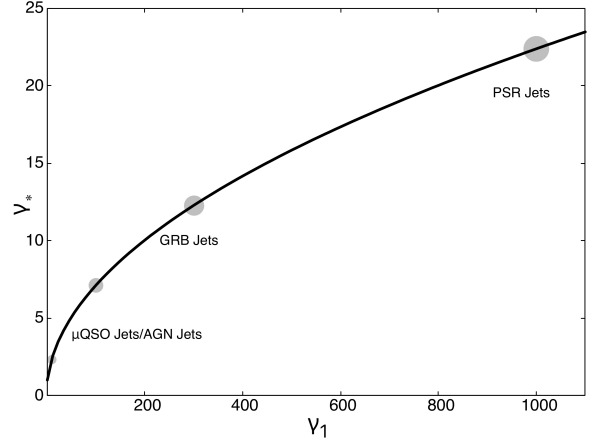


Fig. 3. Theoretical Lorentz factor values for jets from different astrophysical sources in the intermediate frame.

5.3. Growth rate

In the intermediate frame, the growth rate σ of the instability is given as

$$\sigma = \sqrt{gk\mathcal{A}}, \quad (21)$$

where the perturbation modes with larger k grow fast. This trend continues until the magnetic field begins to suppress the growth. Since both the Atwood method and the effective gravity g are unchanged in a certain two fluids system, the growth rate stays unchanged.

The growth rate of $k \approx k_{\text{crit,intermediate}}$ is

$$\sigma_c = \gamma_* \sqrt{gk_{\text{crit,non-relativistic}}\mathcal{A}}, \quad (22)$$

the effect of the relativistic motion leads to a larger threshold wavenumber k , as well as high growth rates. However, when we observe the system in the lab frame, due to time dilation, these unstable modes appear to grow slower.

6. Astrophysical implications

Our new analytical results of R-RTI above have indeed been clearly and correctly achieved in the understanding of the properties of the evolution of RTI in relativistic regimes. We think it's very interesting to apply it to the jets observed in different classes of astrophysical sources, such as active galactic nuclei (AGN), microquasars (μ QSO), gamma-ray bursts (GRB), and so on. This made it possible to explain the observation results using the theoretical analysis. Thus, we plot the theoretical Lorentz factors of different jets in the intermediate frame according to equation 14 in Fig. 3. For AGN jets, the mean Lorentz factor ranges from about 10-100 (Hovatta et al. 2009). For GRB jets, $\gamma \sim 10^2$ (Rees & Meszaros 1994), here we take about 300 (Beskin 2010). For jets in microquasars and radio pulsars, the mean Lorentz factor is about 1000 (Beskin 2010). Fig. 3 shows that actually, the relativistic jets with different high Lorentz factors have relatively small relativistic effects in the intermediate frame. Both AGN jets and GRB jets have Lorentz factor sizes below 15 in the intermediate frame, which means it's difficult for jets to reach the high Lorentz factor in the intermediate frame. To study the growth of R-RTI in jets from different astrophysical sources, we treat the dispersion relation in equation 16 as dimensionless and then plot the stability boundary of R-RTI in Fig. 4. We find that the high Lorentz factors of jets increase the effective inertia of

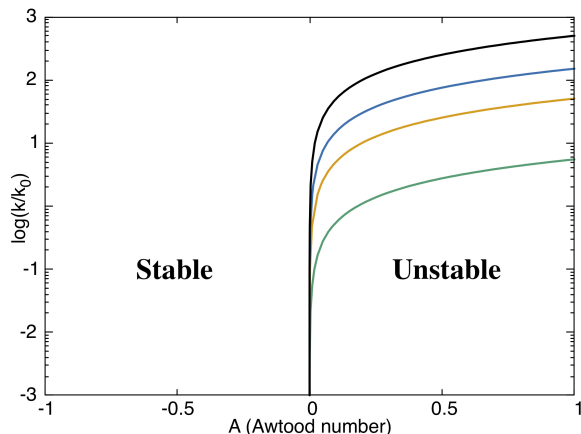


Fig. 4. Stability boundary of R-RTI in different jets in the intermediate frame. The lines above are the boundaries of the onset of R-RTI in jets with different Lorentz factors. The X-axis and Y-axis are the dimensionless Atwood number and the logarithms of wave number respectively. The green and yellow lines show the "zero-line" ($\frac{\omega^2}{gk} = 0$) of R-RTI in AGN jets. The blue one and black one are the "zero-line" of R-RTI in GRB jets and PSR/ μ QSO jets, respectively. The $k_0 = \frac{2\pi g(\rho_1 h_1 - \rho_2 h_2)}{\mu B^2}$ is the critical wavenumber in non-relativistic regime.

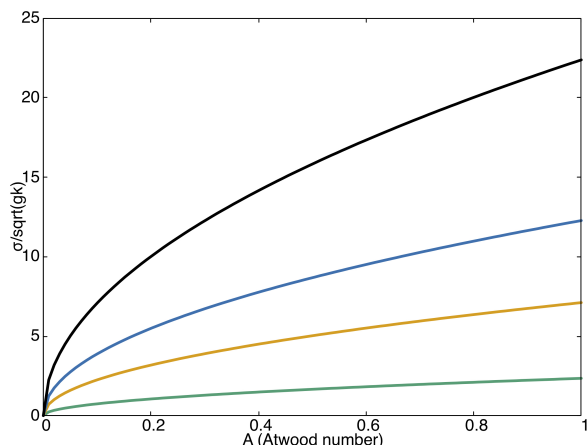


Fig. 5. The dimensionless growth rates of the R-RTI. The green, yellow, blue, and black lines show the analytical relation between the Atwood number and dimensionless growth rates σ/\sqrt{gk} in Eq. 22 with different Lorentz factors $\gamma_1 = 10, 100, 300, 1000$, respectively.

the gas, enabling the growth of small-scale perturbations in R-RTI. Compared to AGN jets and GRB jets, the higher Lorentz factor allows the smaller scale perturbations to be the onset of R-RTI. The horizontal magnetic field here plays a role in suppressing the growth of instability.

We also compare the growth rates of R-RTI in the jets from different sources. Fig.5 shows the high growth rates for jets with large Lorentz factors, which means the instability grows fast in the superfast jets. The density contrast between the jet and ambient medium is also an important reason for the growth rates, thus, the effect of the density ratio of jet and medium η on the growth of instability is extensively studied in many numerical simulations.

7. Conclusions and discussions

The Relativistic Rayleigh–Taylor Instability (R-RTI) is expected to occur in astrophysical jets from different sources, e.g. AGNs and GRBs. We present the correct form of the linear theory of the evolution of relativistic R-RTI in the magnetized medium. By introducing the concept of an "intermediate frame" where the two fluids move toward opposite directions with common Lorentz factors, we propose a procedure to address the inconsistencies in the previous derivations without redoing them. This intermediate frame is a convenient frame of choice to understand the relativistic effects.

Whether R-RTI can develop is determined by the relativistic Atwood number. We find that under relativity, the Atwood number retains the original form

$$\mathcal{A} = \frac{\rho_1 h_1 - \rho_2 h_2}{\rho_1 h_1 + \rho_2 h_2}.$$

contains no apparent relativistic correlations. Thus, the development of R-RTI is determined only by density contrast. The effect of the relativistic motion is to weaken the suppressing effect of the magnetic field on the growth of R-RTI. This in turn allows small perturbations that are otherwise stable to grow. In reality, one should also consider the following *apparent* effects: In the rest frame of the black hole, the instability grows slower because of the time dilation and the eddies procured by the instability should appear much smaller due to length contraction.

The astrophysical jets are complex systems where the magnetic field can organize in several different ways, and other instabilities, such as the Kelvin–Helmholtz instability (KHI) can also occur. Nevertheless, our results of the development of R-RTI in the linear regime set up the function upon which understanding of these complex systems can be established.

Future work on relativistic fluid dynamics will be crucial for understanding more complex astrophysical systems. As observational capabilities improve, incorporating non-linear effects and exploring interactions between different instabilities will be key. This ongoing research will deepen our understanding of phenomena such as black hole accretion, cosmic jets, and compact object formation, cementing the importance of relativistic hydrodynamics in astrophysics.

Acknowledgements. QJ and CBS are supported by the National Natural Science Foundation of China (NSFC) under grant No. 12073021. GXL is supported by the NSFC under grants No. 12273032 and 12033005. We thank Prof. Martin Pohl for proofreading this paper and wise comments.

References

- Matsumoto, J., Aloy, M. A., & Perucho, M. 2017, Monthly Notices of the Royal Astronomical Society, 472, 1421–1431, doi:10.1093/mnras/stx2012
- Rees, M. J., & Meszaros, P. 1994, The Astrophysical Journal Letters, 430, L93, doi:10.1086/187446
- Wilder, R. L., & Richtmyer, R. D. 1954, Physics Today, 7, 18, doi:10.1063/1.3061540
- Toma, K., Komissarov, S. S., & Porth, O. 2017, Monthly Notices of the Royal Astronomical Society, 472, 1253–1258, doi:10.1093/mnras/stx1770
- Chandrasekhar, S. 1961, Hydrodynamic and Hydromagnetic Stability (Oxford University Press)
- Perucho, M. 2019, Galaxies, 7, 70, doi:10.3390/galaxies7030070
- Sharp, D. H. 1984, Physica D: Nonlinear Phenomena, 12, 3, doi:10.1016/0167-2789(84)90510-4
- Wang, C.-Y., & Chevalier, R. A. 2001, The Astrophysical Journal, 549, 1119–1134, doi:10.1086/319439
- Gourgoulias, K. N., & Komissarov, S. S. 2018, Monthly Notices of the Royal Astronomical Society, 475, L125–L129, doi:10.1093/mnras/sly016
- Frascetti, F., Teyssier, R., Ballet, J., & Decourchelle, A. 2010, Astronomy & Astrophysics, 515, A104, doi:10.1051/0004-6361/200912692

- Zhdankin, V., Ripperda, B., & Philippov, A. A. 2023, *Physical Review Research*, 5, 043023, doi:[10.1103/PhysRevResearch.5.043023](https://doi.org/10.1103/PhysRevResearch.5.043023)
- Zhdankin, V., Ripperda, B., & Philippov, A. 2023, *AAS/High Energy Astrophysics Division*, 55, 116.66
- Hillier, A. S. 2016, *Monthly Notices of the Royal Astronomical Society*, 462, 2256–2265, doi:[10.1093/mnras/stw1805](https://doi.org/10.1093/mnras/stw1805)
- Hillier, A. 2018, *Reviews of Modern Plasma Physics*, 2, 1, doi:[10.1007/s41614-017-0013-2](https://doi.org/10.1007/s41614-017-0013-2)
- Rigon, G., Albertazzi, B., Mabey, P., et al. 2021, *Physical Review E*, 104, 045213, doi:[10.1103/PhysRevE.104.045213](https://doi.org/10.1103/PhysRevE.104.045213)
- Hovatta, T., Valtaoja, E., Tornikoski, M., & Lähteenmäki, A. 2009, *Astronomy & Astrophysics*, 494, 527–537, doi:[10.1051/0004-6361:200811150](https://doi.org/10.1051/0004-6361/200811150)
- Beskin, V. S. 2010, *Physics Uspekhi*, 53, 1199–1233, doi:[10.3367/UFNe.0180.201012b.1241](https://doi.org/10.3367/UFNe.0180.201012b.1241)
- Kane, J., Drake, R. P., & Remington, B. A. 1999, *The Astrophysical Journal*, 511, 335–340, doi:[10.1086/306685](https://doi.org/10.1086/306685)
- Landau, L. D., & Lifshitz, E. M. 1987, *Fluid Mechanics* (Pergamon Press)
- Taylor, E. F., & Wheeler, J. A. 1992, *Spacetime Physics: An Introduction to Special Relativity* (W. H. Freeman)

Appendix A: Derivation of the dispersion relation of R-RTI

Fig. 1 shows the jet and ambient medium which is separated by one interface, with different densities and Lorentz factor, ρ_1, ρ_2 and γ_1, γ_2 , respectively. Here, we add one uniform horizontal magnetic field along the x axis. g is effective acceleration.

Here, we treat the two-fluid system as an ideal gas then we have the basic equations of relativistic magneto-hydrodynamics:

$$\frac{\partial(\gamma\rho)}{\partial t} + \nabla \cdot (\gamma\rho\mathbf{v}) = 0, \quad (\text{A.1})$$

$$\gamma^2\rho h \left[\frac{\partial\mathbf{v}}{\partial t} + (\mathbf{v} \cdot \nabla)\mathbf{v} \right] = -\nabla P - \frac{\mathbf{v}}{c^2} \frac{\partial P}{\partial t} + \gamma^2\rho h\mathbf{g} + \mu\mathbf{J} \times \mathbf{B}, \quad (\text{A.2})$$

$$\nabla \cdot \mathbf{B} = 0, \quad (\text{A.3})$$

$$\frac{\partial\mathbf{B}}{\partial t} = \nabla \times (\mathbf{v} \times \mathbf{B}). \quad (\text{A.4})$$

Eq. A.1 is the continuity Eq. A.2 is the momentum Eq. ρ is the rest-mass density, \mathbf{B} is the magnetic field applied along the x direction, γ is the Lorentz factor, \mathbf{v} is a velocity vector, P is total pressure including gas pressure P_{gas} and magnetic pressure, $P = P_{\text{gas}} + \frac{B^2}{2\gamma^2} + \frac{(v\cdot\mathbf{B})^2}{2}$, \mathbf{g} is acceleration vector, h is specific enthalpy including the contribution of gas and magnetic field, the total specific enthalpy is defined as $h = h_{\text{gas}} + \frac{B^2}{\gamma^2\rho} + \frac{(v\cdot\mathbf{B})^2}{\rho}$.

The gas enthalpy is defined as $h_{\text{gas}} = 1 + \frac{\Gamma}{\Gamma-1} \frac{P}{\rho c^2}$.

Then we add perturbations. The $\delta\rho$, δP , $\delta\mathbf{B}$ are density perturbations, pressure perturbations, and magnetic perturbations, respectively. We substitute $\rho + \delta\rho$, $P + \delta P$, $\mathbf{B} + \delta\mathbf{B}$ and $\delta\mathbf{v}$ into Eq. A.1–A.4, and we ignore all high-order terms and then obtain a set of perturbed equations:

$$\frac{\partial}{\partial t}(\gamma\delta\rho) + \gamma\rho\nabla \cdot \delta\mathbf{v} = 0, \quad (\text{A.5})$$

$$\gamma^2\rho h \left[\frac{\partial}{\partial t}\delta\mathbf{v} + (\mathbf{v} \cdot \nabla)\delta\mathbf{v} \right] = -\nabla\delta P + \gamma^2\rho h\mathbf{g} + \frac{4\pi}{\mu} [(\nabla \times \mathbf{B}) \times \delta\mathbf{B} + (\nabla \times \delta\mathbf{B}) \times \mathbf{B}], \quad (\text{A.6})$$

$$\nabla \cdot \delta\mathbf{B} = 0, \quad (\text{A.7})$$

$$\frac{\partial}{\partial t}(\delta\mathbf{B}) = \nabla \times (\delta\mathbf{v} \times \mathbf{B}). \quad (\text{A.8})$$

where B denotes the strength of a uniform horizontal magnetic field along the x -direction. $\delta\mathbf{B}$ is the perturbation which contains two components $\delta\mathbf{B} = (\delta B_x, \delta B_y, 0)$. The velocity components $\delta\mathbf{v} = (\delta v_x, \delta v_y, 0)$. This also means that we expand it in two dimensions to the x - y plane and get a set of linearized equations

$$\frac{\partial}{\partial t}(\gamma\delta\rho) + \gamma\rho \left(\frac{\partial}{\partial x}\delta v_x + \frac{\partial}{\partial y}\delta v_y \right) = 0, \quad (\text{A.9})$$

$$\gamma^2\rho h \left[\frac{\partial}{\partial t}\delta v_x + v_x \frac{\partial}{\partial x}\delta v_x + v_y \frac{\partial}{\partial y}\delta v_x \right] = -\frac{\partial}{\partial x}\delta P + \frac{4\pi}{\mu} \left[-\frac{\partial B_x}{\partial y}\delta B_y + \frac{\partial \delta B_y}{\partial x} \cdot B_y \right], \quad (\text{A.10})$$

$$\gamma^2\rho h \left[\frac{\partial}{\partial t}\delta v_y + v_x \frac{\partial}{\partial x}\delta v_y + v_y \frac{\partial}{\partial y}\delta v_y \right] = -\frac{\partial}{\partial y}\delta P + \gamma^2\rho h\mathbf{g} + \frac{4\pi}{\mu} \left[\frac{\partial B_y}{\partial x}\delta B_x - \frac{\partial B_x}{\partial x} \cdot \delta B_y \right], \quad (\text{A.11})$$

$$\frac{\partial}{\partial x}\delta B_x + \frac{\partial}{\partial y}\delta B_y = 0, \quad (\text{A.12})$$

$$\frac{\partial}{\partial t}(\delta B_x) = \frac{\partial}{\partial y}(v_y B_x - v_x B_y), \quad (\text{A.13})$$

$$\frac{\partial}{\partial t}(\delta B_y) = \frac{\partial}{\partial x}(v_x B_y - v_y B_x), \quad (\text{A.14})$$

Here, we consider the normal mode perturbations for different physical quantities:

$$\delta\rho, \delta P, \delta\mathbf{B}, \delta\mathbf{v} \propto \exp i(kx - \omega t), \quad (\text{A.15})$$

We insert these small perturbations into the linearized Eqs. A.9–A.14, we obtain

$$-i\omega\gamma\delta\rho + \gamma\rho(ik\delta v_x + v_y D_y \delta v_y) = 0, \quad (\text{A.16})$$

$$\gamma^2\rho h [-i\omega\delta v_x + ikv_x\delta v_x + v_y D_y \delta v_x] = -ik\delta P + \frac{4\pi}{\mu} [-D_y B_x \delta B_y + ik\delta B_y B_y], \quad (\text{A.17})$$

$$\gamma^2\rho h [-i\omega\delta v_y + ikv_x\delta v_y + v_y D_y \delta v_y] = -D_y \delta P + \gamma^2\rho h\mathbf{g} + \frac{4\pi}{\mu} [D_x B_y \delta B_x - D_x B_x \delta B_y], \quad (\text{A.18})$$

$$ik\delta B_x + D_y \delta B_y = 0, \quad (\text{A.19})$$

$$-i\omega\delta B_x = D_y(v_y B_x - v_x B_y), \quad (\text{A.20})$$

$$-i\omega\delta B_y = D_x(v_x B_y - v_y B_x). \quad (\text{A.21})$$

Here, we have $D_x = \frac{\partial}{\partial x}$ and $D_y = \frac{\partial}{\partial y}$. Combining Eqs. A.16–A.21, after eliminating the small perturbations $\delta\rho$, δP , $\delta\mathbf{B}$, we obtain

$$\begin{aligned} \frac{\partial}{\partial y}(\gamma^2\rho h \frac{\partial}{\partial y}\delta v_y) + \frac{\mu B^2 k^2}{4\pi\omega^2} \left(\frac{\partial^2}{\partial y^2} - k^2 \right) \delta v_y - k^2 \gamma^2 \rho h \delta v_y \\ = -\gamma^2 h \frac{gk^2}{\omega^2} \delta v_y \frac{\partial}{\partial y} \rho. \end{aligned} \quad (\text{A.22})$$

We assume that there are two different uniform fluids separated by a horizontal boundary at $y = 0$, whose densities are ρ_1 , ρ_2 , we obtain

$$\left(\frac{\partial^2}{\partial y^2} - k^2\right)\delta v_y = 0, \quad (\text{A.23})$$

where the general solution is

$$\delta v_y = Ae^{+ky} + Be^{-ky}, \quad (\text{A.24})$$

$$\delta v_y = Ae^{+ky} (y < 0), \quad (\text{A.25})$$

$$\delta v_y = Ae^{-ky} (y > 0). \quad (\text{A.26})$$

We have chosen the same constant A in the upper solutions for regions of $y > 0$ and $y < 0$, ensuring the smooth continuity of velocity δv_y through the boundary at $y = 0$. We plug the above solutions into Eq. A.22 and integrate them across the interface. Finally, we obtain the following dispersion relation of magnetized R-RTI,

$$\omega^2 = -gk \left\{ \frac{\gamma_1^2 \rho_1 h_1 - \gamma_2^2 \rho_2 h_2}{\gamma_1^2 \rho_1 h_1 + \gamma_2^2 \rho_2 h_2} - \frac{\mu B^2 k}{2\pi (\gamma_1^2 \rho_1 h_1 + \gamma_2^2 \rho_2 h_2) g} \right\}. \quad (\text{A.27})$$

We use the footmarks 1 and 2 to denote the variables in the upper and lower fluids, respectively. The instability sets in when $\omega^2 < 0$ (Chandrasekhar 1961). The temporal growth rate of R-RTI, σ is defined as the imaginary part of the frequency:

$$\sigma = \text{Im } \omega. \quad (\text{A.28})$$

The dimensionless growth rate is given by

$$\frac{\sigma}{\sqrt{gk}} = \sqrt{\mathcal{A}}. \quad (\text{A.29})$$

where \mathcal{A} is the Atwood number, which is a very important dimensionless parameter in fluid dynamics that describes the linear growth of the instabilities. We obtain the classical non-magnetic relativistic Atwood number from Eq. A.27

$$\mathcal{A} = \frac{\gamma_1^2 \rho_1 h_1 - \gamma_2^2 \rho_2 h_2}{\gamma_1^2 \rho_1 h_1 + \gamma_2^2 \rho_2 h_2}. \quad (\text{A.30})$$

For the second magnetic term in Eq. A.27, we note that the perturbations with $k = 0$, and the magnetic field have no effects on the growth of R-RTI.